



*Supplement of*

## **Highly stratified mid-Pliocene Southern Ocean in PlioMIP2**

**Julia E. Weiffenbach et al.**

*Correspondence to:* Julia E. Weiffenbach ([j.e.weiffenbach@uu.nl](mailto:j.e.weiffenbach@uu.nl))

The copyright of individual parts of the supplement might differ from the article licence.

## Supplementary Tables and Figures

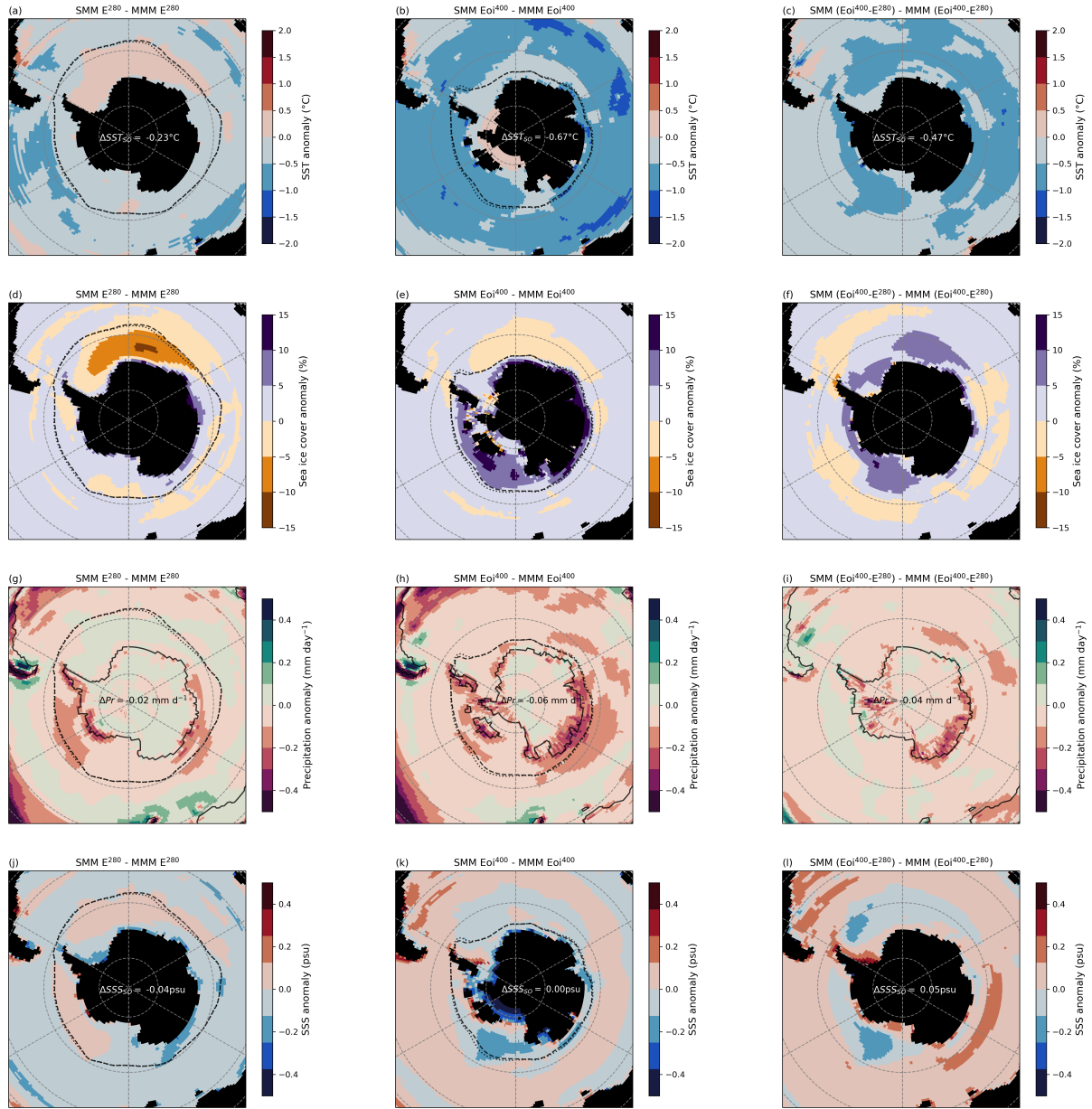


**Figure S1.** (a)-(c) SMM-MMM sea surface temperature (SST) anomalies for E<sup>280</sup>, Eoi<sup>400</sup> and Eoi<sup>400</sup>-E<sup>280</sup>, respectively. Dotted and dashed lines show the SMM and MMM sea-ice edge (15% sea-ice cover). The Southern-Ocean-average SST anomaly is printed. (d)-(f) SMM-MMM sea-ice cover anomalies for E<sup>280</sup>, Eoi<sup>400</sup> and Eoi<sup>400</sup>-E<sup>280</sup>, respectively. (g)-(i) Same as (a)-(c) for precipitation. The percentage change printed in (g), (h) and (i) is with respect to the MMM E<sup>280</sup>, MMM Eoi<sup>400</sup> and MMM Eoi<sup>400</sup>-E<sup>280</sup> precipitation, respectively. (j)-(l) Same as (a)-(c) for sea surface salinity (SSS).

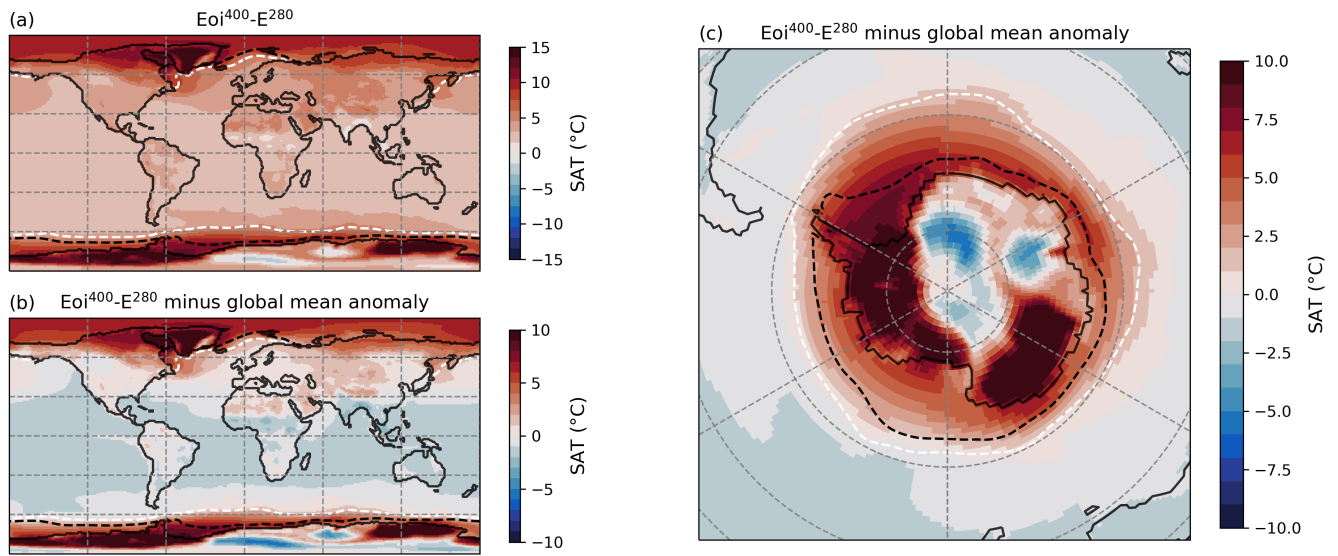


**Figure S2.** (a) MMM Eoi<sup>400</sup>-E<sup>280</sup> surface air temperature (SAT) anomaly. (b) MMM Eoi<sup>400</sup>-E<sup>280</sup> SAT anomaly minus the MMM global mean SAT anomaly. (c) Same as (b) but on an orthographic projection centered in Antarctica. White and black dashed lines show the MMM sea-ice edge (15% sea-ice cover) in E<sup>280</sup> and Eoi<sup>400</sup>, respectively.

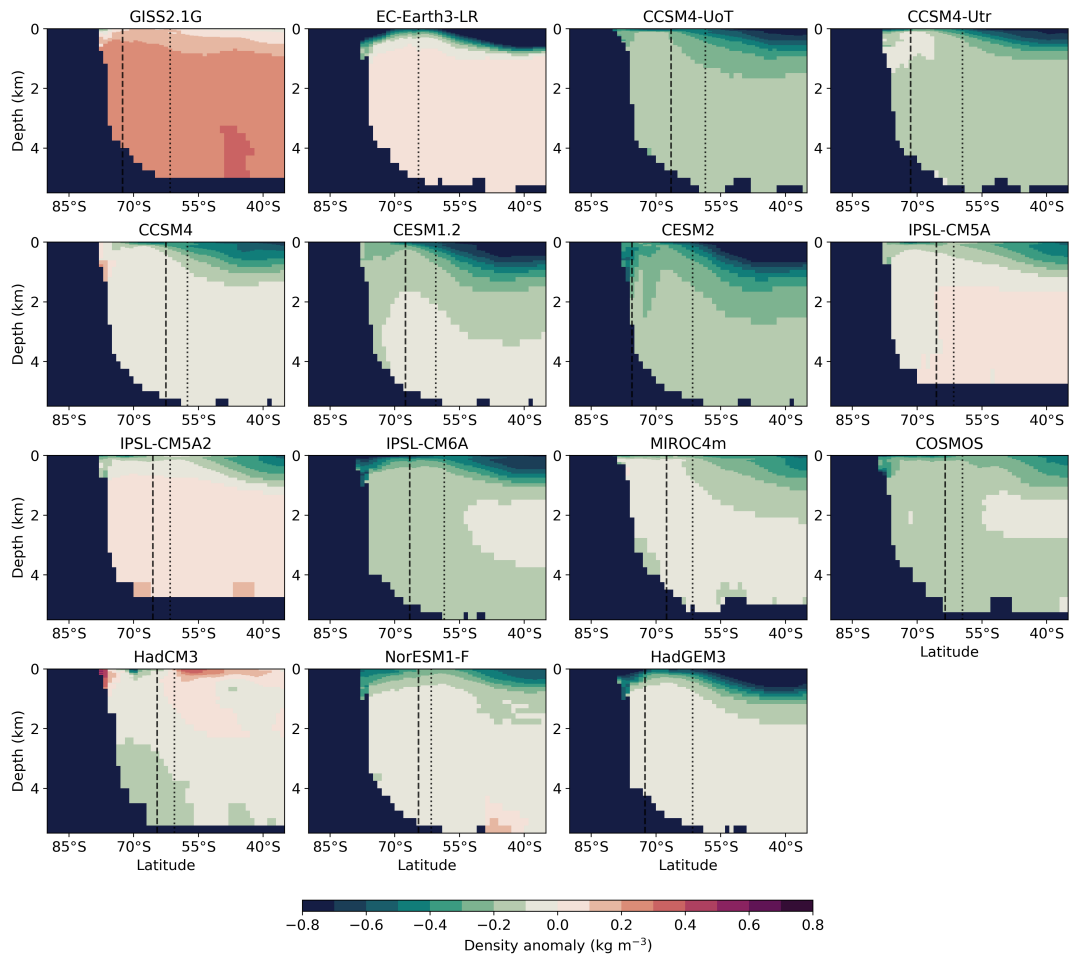


**Figure S3.** Individual model  $E_{oi}^{400}-E^{280}$  potential density anomalies. Vertical dotted and dashed lines indicate the MMM zonal mean sea-ice edge (15% sea-ice cover) in  $E^{280}$  and  $E_{oi}^{400}$ , respectively.

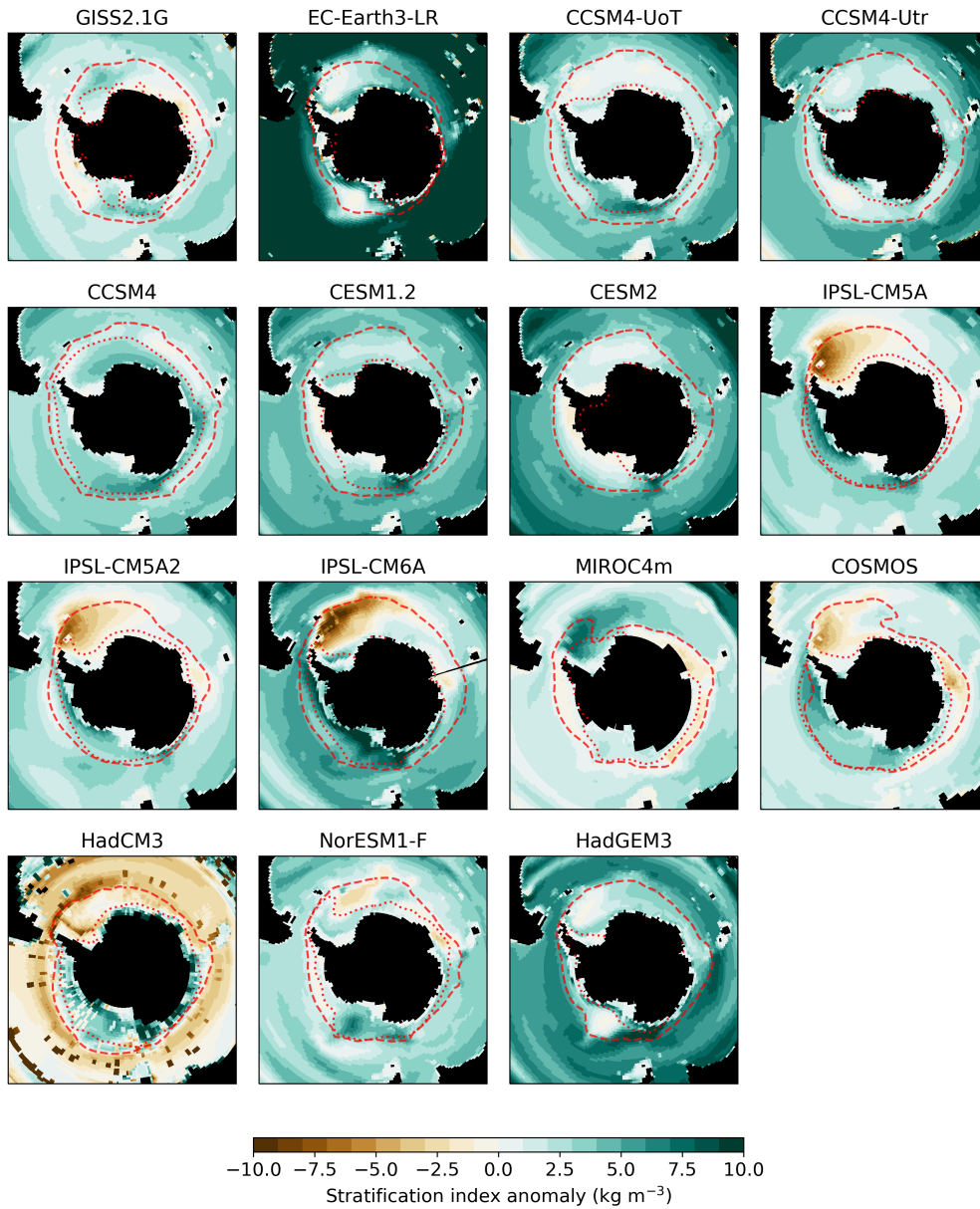


**Figure S4.** Individual model  $E_{oi}^{400} - E^{280}$  stratification index anomalies. Red dashed and dotted lines show the MMM sea-ice edge (15% sea-ice cover) in  $E^{280}$  and  $E_{oi}^{400}$ , respectively. The stratification index is calculated for each grid cell according to Equation 1.

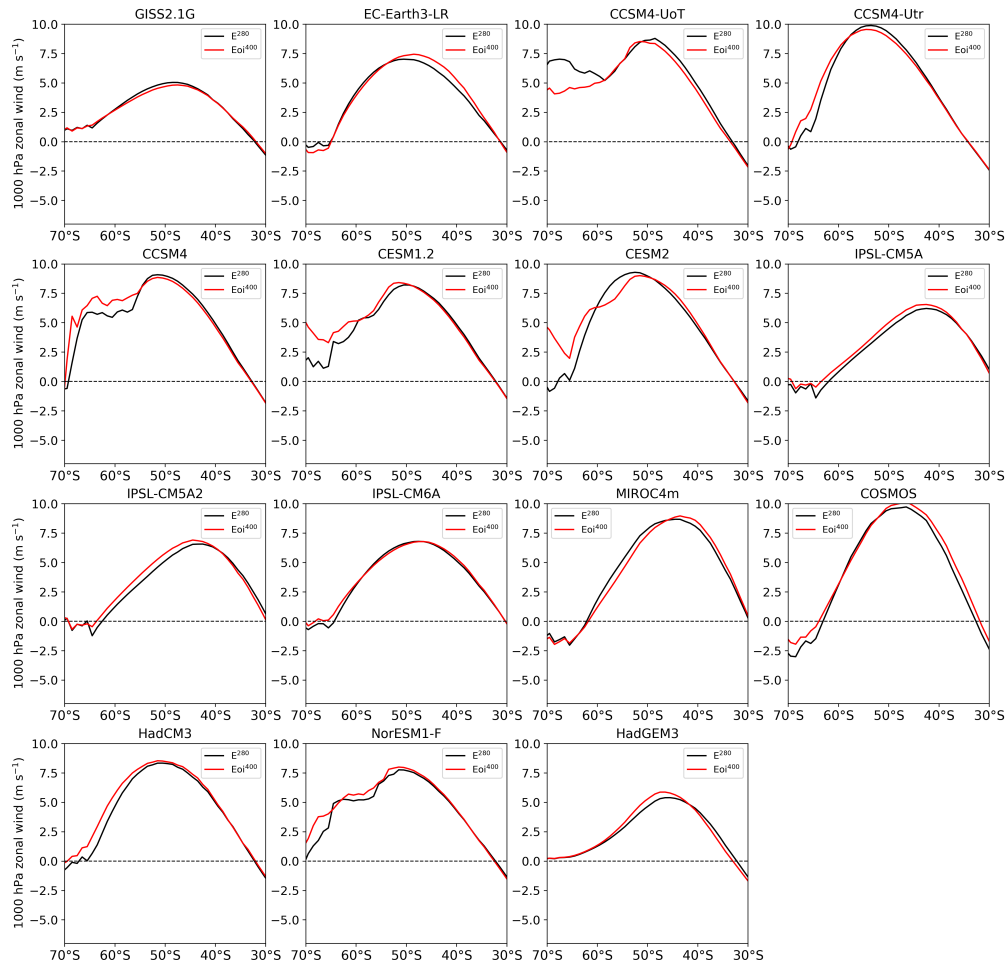


**Figure S5.** Individual model  $E_{01}^{400}$  and  $E^{280}$  zonal-mean 1000 hPa zonal wind.

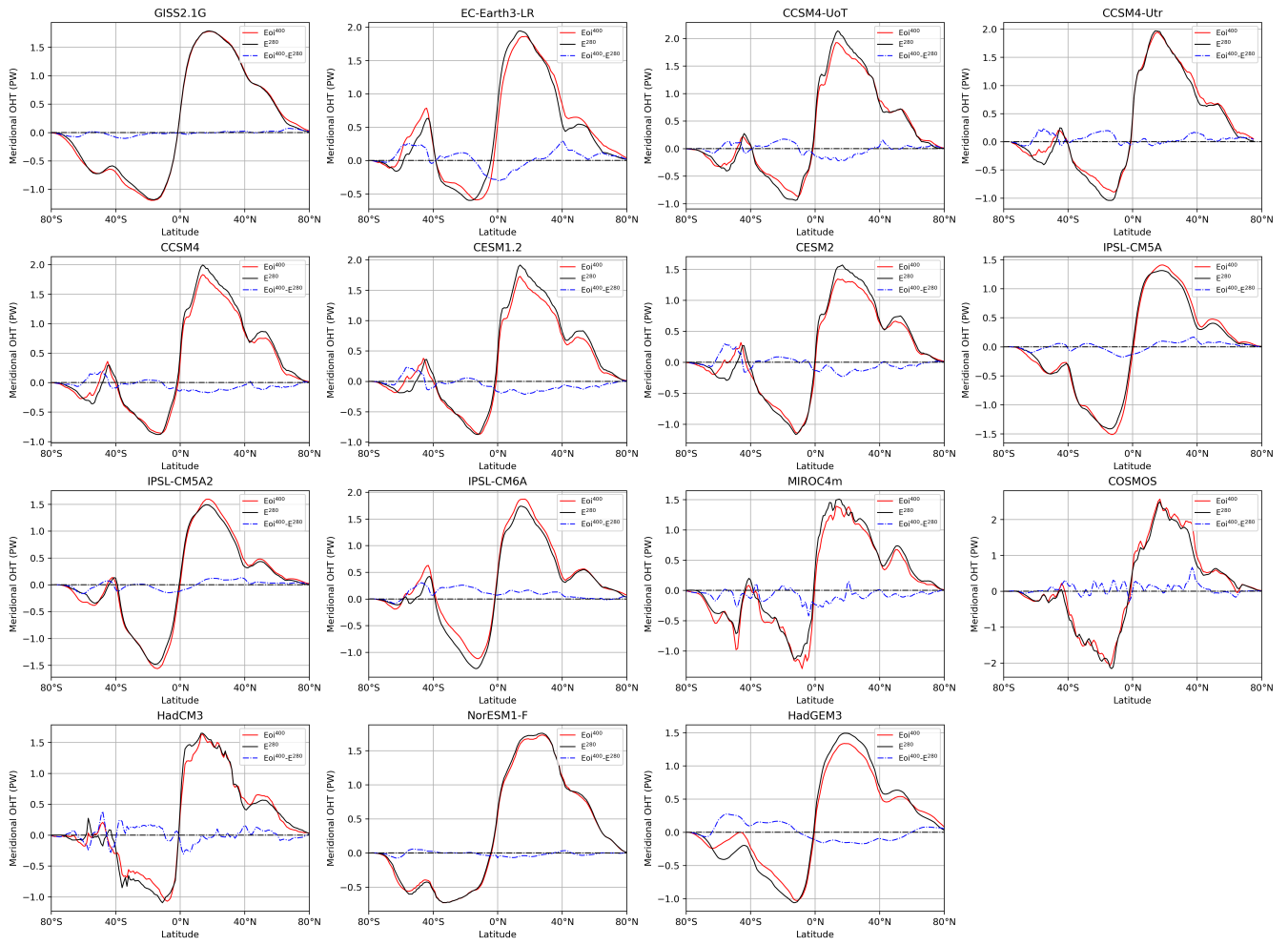


**Figure S6.** Individual model meridional ocean heat transport for  $E^{280}$ ,  $E_{oi}^{400}$  and  $E_{oi}^{400} - E^{280}$ .



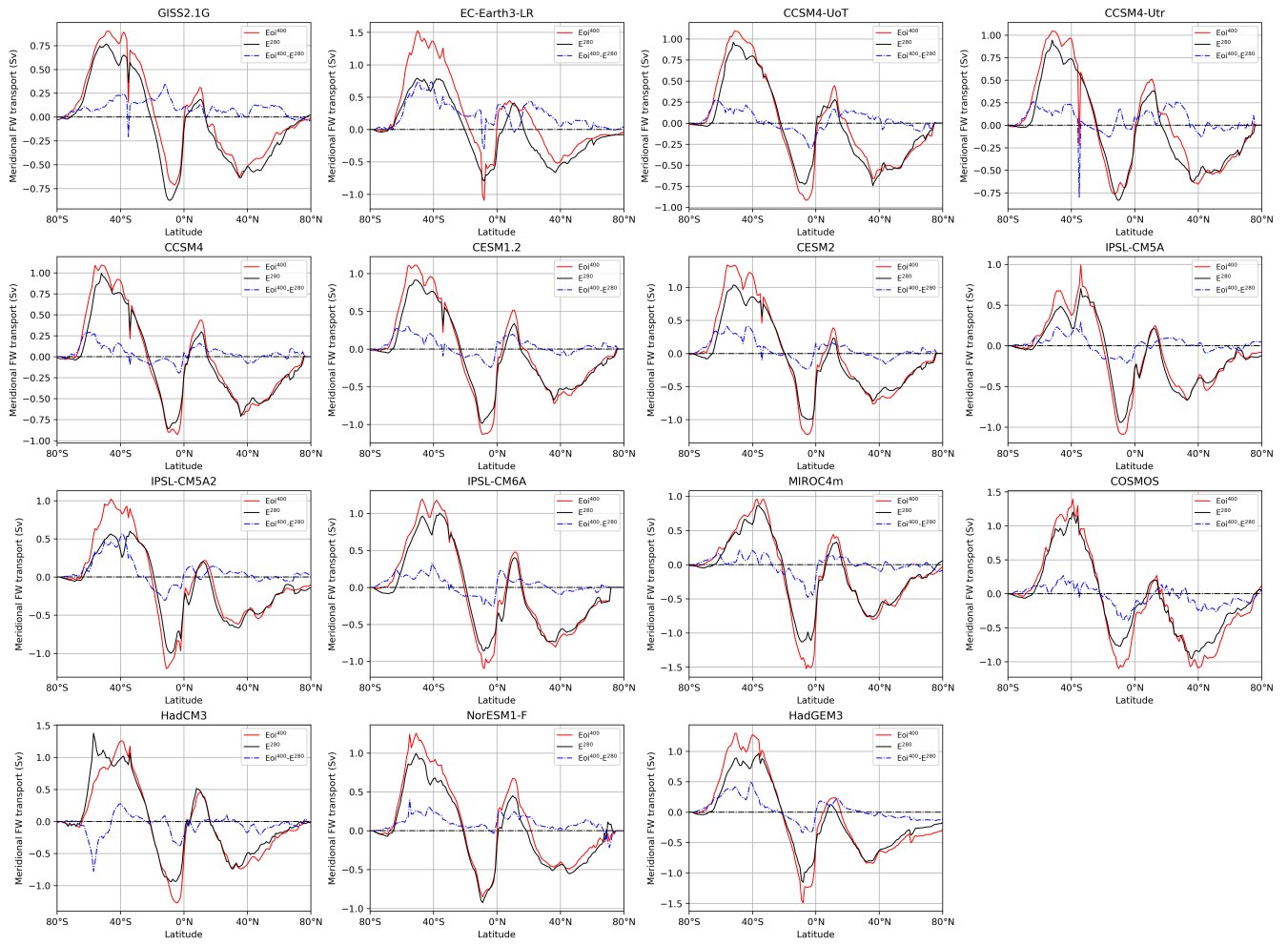


**Figure S7.** Individual model meridional freshwater transport for  $E^{280}$ ,  $E_{oi}^{400}$  and  $E_{oi}^{400}-E^{280}$ .

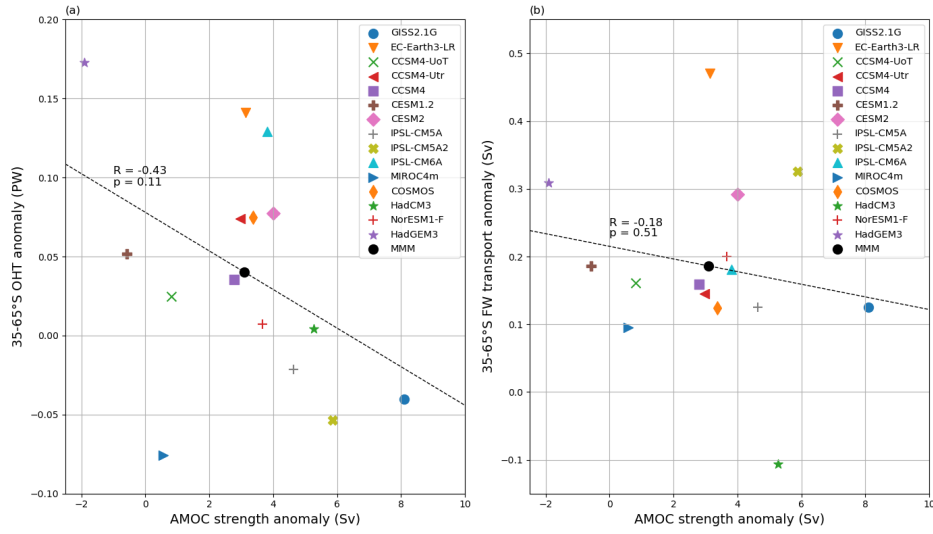


**Figure S8.** (a) Scatter plot of the individual model  $E_{oi}^{400}-E^{280}$  AMOC cell strength anomaly against the 35-65°S-average global ocean heat transport (OHT) anomaly. (b) Scatter plot of the individual model  $E_{oi}^{400}-E^{280}$  AMOC cell strength anomaly against the 35-65°S-average global freshwater transport (FWT) anomaly. Dashed lines show a linear least-squares fit to the individual model data, with indicated correlation  $R$ - and  $p$ -values.

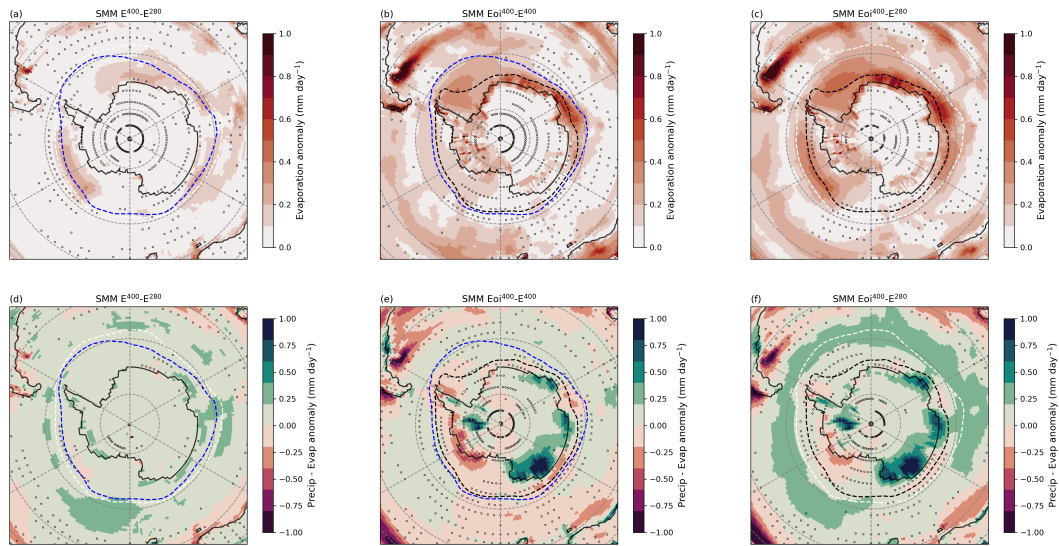


**Figure S9.** (a) SMM  $E^{400}-E^{280}$  precipitation minus evaporation (PmE) anomaly. (b),(c) Same as (a) for  $Eoi^{400}-E^{400}$  and  $Eoi^{400}-E^{280}$ . White, blue and black dashed lines show the SMM sea-ice edge (15% sea-ice cover) in  $E^{280}$ ,  $E^{400}$  and  $Eoi^{400}$ , respectively. Stippling indicates that less than 5 out of 7 (<70%) of the models included in the SMM agree on the sign of change.

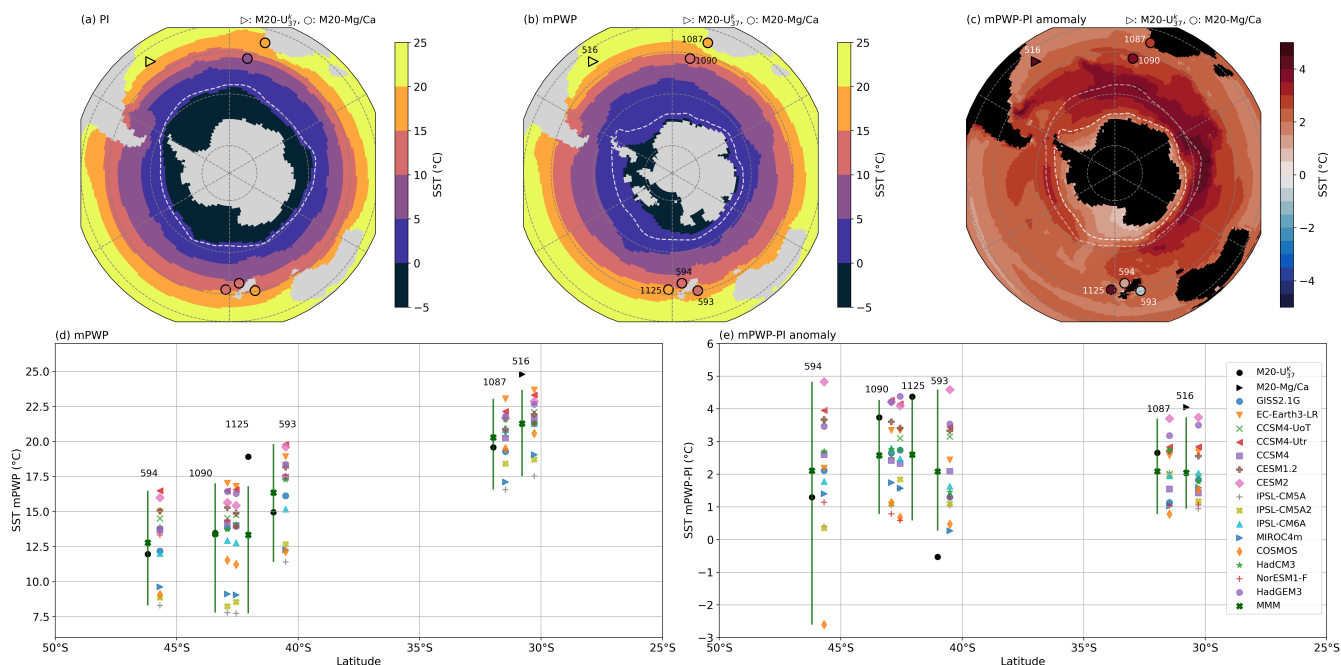


**Figure S10.** (a) Southern Ocean MMM  $E^{280}$  SST and pre-industrial ERSSTv5 SSTs (Huang et al., 2017) at proxy locations. (b) Southern Ocean MMM  $E_{oi}^{400}$  SST and KM5c mPWP SSTs reconstructed by McClymont et al. (2020) (M20) at proxy locations. M20- $U_{37}^k$  and M20-Mg/Ca refer to the McClymont et al. (2020) SST reconstructions using  $U_{37}^k$  and Mg/Ca proxies, respectively. (c) Southern Ocean MMM  $E_{oi}^{400}-E^{280}$  SST anomalies and KM5c mPWP SSTs (McClymont et al., 2020) minus pre-industrial ERSSTv5 SSTs (Huang et al., 2017) at proxy locations. (d) Individual model mPWP ( $E_{oi}^{400}$ ) SSTs and reconstructed mPWP SSTs (black) at proxy locations in or near the Southern Ocean. A vertical dark green line shows the model spread and the MMM is indicated by a dark green cross. (e) Individual model SST anomalies ( $E_{oi}^{400}-E^{280}$ ) and reconstructed mPWP-Pi SST anomalies (black) at proxy locations in or near the Southern Ocean. A vertical dark green line shows the model spread and the MMM is indicated by a dark green cross. Pre-industrial SSTs are computed with the pre-industrial ERSST5 1870-1900 data (Huang et al., 2017).

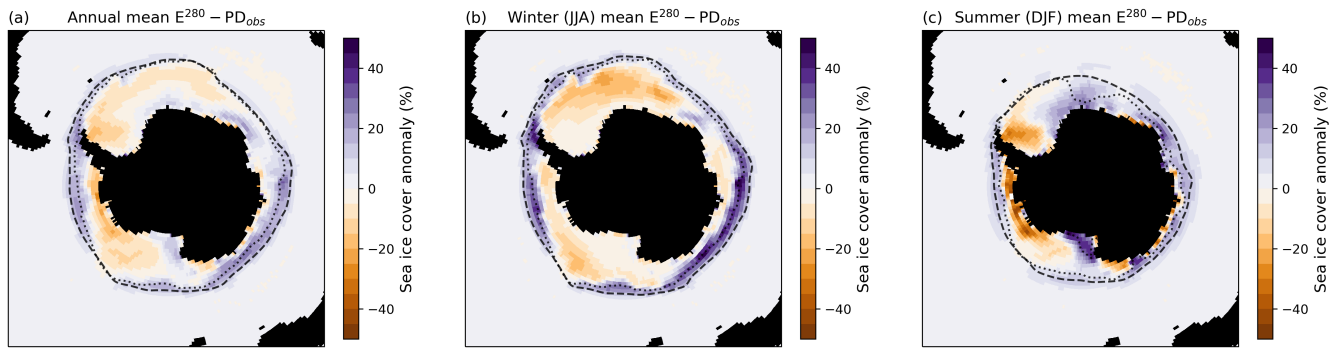


**Figure S11.** (a) Annual-mean MMM  $E^{280}$  – observed present-day (PD<sub>obs</sub>, 1979-1999) sea-ice cover anomaly. (b) Winter-mean (JJA) MMM  $E^{280}$  – observed present-day (PD<sub>obs</sub>, 1979-1999) sea-ice cover anomaly. (c) Summer-mean (DJF) MMM  $E^{280}$  – observed PD (1979-1999) sea-ice cover anomaly. Black dashed lines show the MMM  $E^{280}$  sea-ice edge (15% sea-ice cover) and black dotted lines show the PD<sub>obs</sub> sea-ice edge.

**Table S1.** Individual model, MMM and SMM stratification index averaged over the high-latitude Southern Ocean (60–90°S).

Model	Average stratification index 60–90°S ( $\text{kg m}^{-3}$ )				
	$E^{280}$	$E^{400}$	$E_{oi}^{400}$	$E_{oi}^{400} - E^{280}$	$E^{400} - E^{280}$
GISS-E2.1G	4.7		5.4	0.7	
EC-Earth3-LR	5.6		10.2	4.6	
CCSM4-UoT	4.7	5.9	6.2	1.5	1.2
CCSM4-Utr	5.1		6.8	1.7	
CCSM4	5.1		7.2	2.1	
CESM1.2	7.0		8.9	1.9	
CESM2	7.9	8.9	9.4	1.5	1.0
IPSL-CM5A	3.3		4.9	1.6	
IPSL-CM5A2	3.8	4.1	5.1	1.3	0.3
IPSL-CM6A	5.9		9.0	3.1	
MIROC4m	3.7	3.7	4.5	0.8	0.0
COSMOS	3.5	4.4	5.2	1.7	0.9
HadCM3	6.7	7.5	7.1	0.4	0.8
NorESM1-F	5.1	5.9	6.8	1.7	0.8
HadGEM3	4.7		8.5	3.8	
MMM	5.1		7.0	1.9	
SMM	5.1	5.8	6.3	1.2	0.7